Study on the Transferability of Rolling with Ordered Texturing Roll

Yasuyuki Fujii, Yasushi Maeda, and Hiroshi Utsunomiya

Abstract Surface textured rolling is designed to transfer roughness onto the sheet from the surface of textured rolls. The authors investigated the influence of rolling conditions on transferability using an ordered texture roll experimentally. To understand such influence, we compared the rolled surface profiles during the experiments with those during Finite Element Analysis (FEA). However, at reductions greater than 5%, there is a discrepancy, which is believed to be caused by unknown restraint force. As it is difficult to estimate the restraint force with a 3D profile roll, we carried out experimental transformability tests with 3 simpler kinds of ordered texture rolls, namely, (1) RD, (2) TD, and (3) 45-degree groove rolls. In this paper, the apparent friction coefficients were evaluated experimentally with these rolls. The friction coefficients were found to be affected by several metal flows in the roll bite. In conclusion, it is still difficult to estimate the apparent friction coefficient because these metal flows affect each other.

Keywords Texture rolling · Surface roughness · Friction coefficient · Rolling experiment

Y. Fujii (✉)
Mechanical Working Research Section Materials Research Laboratory, KOBE STEEL, LTD., 1 5-5, Takatsukadai, Nishi-ku, Kobe 651-2271, Japan
e-mail: fujii.yasuyuki@kobelco.com

Y. Maeda
Materials Research Laboratory, KOBE STEEL, LTD., 1 5-5, Takatsukadai, Nishi-ku, Kobe 651-2271, Japan
e-mail: maeda.yasushi@kobelco.com

H. Utsunomiya
Division of Materials and Manufacturing Science, Osaka University, 2-1 Yamadaoka, Suita, Osaka 565-0871, Japan
e-mail: uts@mat.eng.osaka-u.ac.jp

G. Daehn et al. (eds.), *Forming the Future*, The Minerals, Metals & Materials Series,
https://doi.org/10.1007/978-3-030-75381-8_201

1 Introduction

The surface property of rolled strip is one of its most important characteristics. In texture rolling, the profile on the textured roll is transferred to that on the strip. In many previous studies, the character of the surface has employed the average roughness such as Ra [1]. Furthermore, numerous studies of skin-pass rolling with dull rolls have mainly discussed this under conditions where there was less than a 5% reduction. For example, Aoki et al. carried out rolling transcription experiments by changing the reduction, roll roughness, and inlet thickness. They reported that the transcribed average roughness on the sheet is dependent on the reduction, the surface pressure, and the shape factor. However, their results only looked at a low reduction region (<5%), and did not examine behavior at a higher reduction region [2]. Some studies have reported on numerical predictions of surface texture. For example, a rolling 2D-FEM simulation using a zooming method was studied by Yukawa et al. [3]. They showed the results of 2D-FEM at a relatively higher reduction region. However, there was no quantitative comparison with experimental results in their report. A simple compression simulation with a solid die using 2D-elastic-plastic FEM was studied by Ike [4]. In his conclusion, the frictional force and the angle of the die wedge were important for the surface profile. However, this model was a simple compression process. In the rolling process, there are relative vertical and horizontal velocities between the die and the material. In our previous research, we took into account the effect of both relative velocities in the rolling process, using the microscopic 3D deformation mode. In our present research, an ordered textured roll was used experimentally, and the profile of the rolled surface was measured as individual transcribed 3D profiles. To predict each individual profile, a 2-step FEA was established. In the first step, the relative velocity between the roll and the material in the roll bite was decided each time using 2D FEM for macroscopic analysis. In the second step, microscopic 3D FEA of the solid die and elastic–plastic material was applied, giving the relative velocity from macroscopic 2D FEA as the time step boundary conditions. Our results showed that, under lower reduction conditions, there was a high degree of agreement between the numerical predictions and the experimental results [5]. However, there was a discrepancy between them at higher reduction region (Fig. 1) [6]. We discovered that it was difficult to estimate the exact value of the material velocity on the microscopic 3D model from the results of 2D-FEM). It is believed that this affects an accurate estimation of the friction coefficient due to the formation of projections and the pattern itself on the roll.

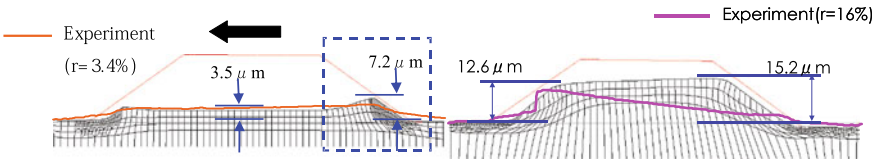

Fig. 1 3D-FEM simulation result (left: r = 3.4%, right: r = 16.0%). (Color figure online)

In this paper, we carried out experiments on transformability with 3 kinds of ordered texture rolls where: (1) the RD groove roll has the groove along the radial direction of the roll, (2) the TD groove roll has the groove along the axial direction of the roll, and (3) the 45-degree groove roll has the groove at an angle of 45° to the roll. We expected that an ordered 3D texture roll might be a mixture of these. These experiments showed that different rolls have different restraint force and friction coefficients.

2 Experimental Conditions

To simplify the discussion, three kinds of work roll with different ordered patterned surfaces were used, as shown in Fig. 2a–c. In Fig. 2a, the RD groove roll has the groove along the cylindrical direction of the roll surface. In Fig. 2b, the TD groove roll has the groove along the axial direction. In Fig. 2c, the 45-degree groove roll has the groove along different 45-degree directions against the center.

These grooves have the same profile as shown in Fig. 3. A 4-high rolling mill was used in the rolling test with these rolls as the work rolls. The back-up roll was 300 mm in diameter, and the work roll 55 mm. The patterned rolls were used as

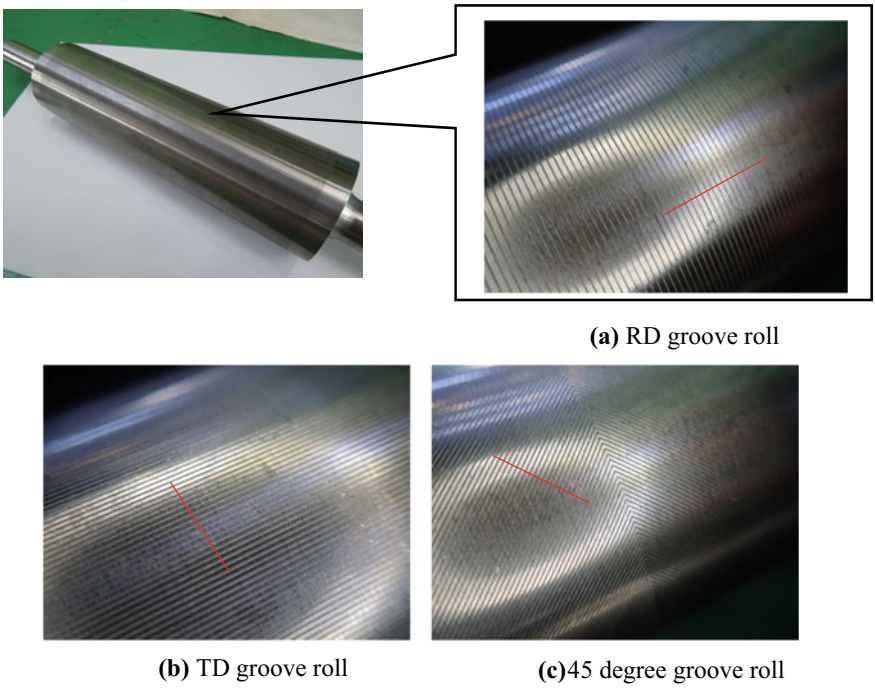

(a) RD groove roll

(b) TD groove roll

(c)45 degree groove roll

Fig. 2 Roll appearance. (Color figure online)

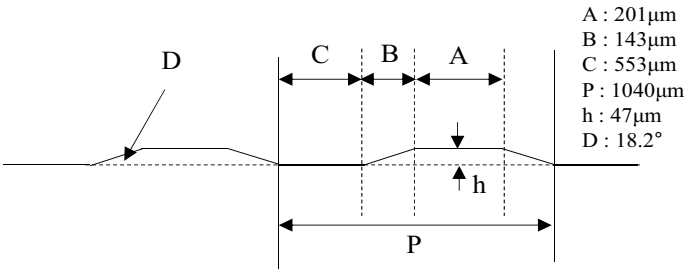

Fig. 3 Roll surface cross section

only the top work roll, and the bottom work roll was set to be a bright roll. The rolled material was pure titanium, 0.61 mm in thickness, 50 mm in width, and about 200 mm in length. The rolling reductions were changed from 5 to 25%. In addition, the 45-degree groove roll was asymmetrical with regard to the direction of rotation. We identified normal rotation and reverse rotation as shown in Fig. 4. A summary of the experimental conditions is shown in Table 1. After the rolling tests, the profiles transcribed onto the surface were measured using a laser microscope.

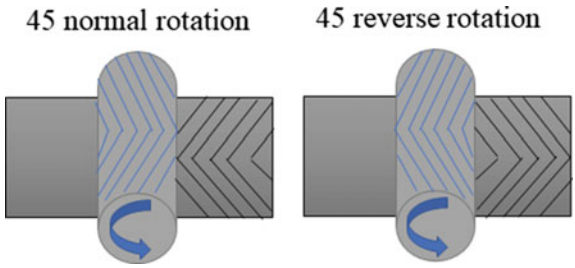

Fig. 4 45-degree groove roll rolling direction. (Color figure online)

Table 1 Experimental conditions

Mill	4Hi
Roll	Upper:groove roll (φ55 mm × L265 mm) (a) RD groove roll (b) TD groove roll (c) 45 degree groove roll Lower:bright (φ55 mm × L265 mm)
Material	Purity titanium (ASME:Gr1) h0.61 mm × w50 mm × L200 mm
Lubricant	Dry
Reduction	5–25%
Tension	0 Mpa
Roll speed	1.0 mpm

3 Experimental Results

3.1 Height of Transcribed Profile

In Fig. 5, the heights of the transcribed profile on the rolled sheets are shown as the relationship of the reductions from the experimental results. The height was strongly dependent on reduction under about 15% with any type of roll. On the other hand, at over 15%, it seems that the height is almost constant, and the values depend on the type of roll. Further, the height of the transcribed profile for each type of roll increases at higher reductions in the following order: TD groove roll, reverse rotation of 45-degree roll, normal rotation of 45-degree roll, RD groove roll. This order is understandable if the following mechanism is assumed, namely, that the height of the profile is formed by compressive metal flow on the surface of the roll bite. In general, material elongates along the rolling direction in the rolling process. In these experiments, surface elongation in the roll bite is resisted by the groove on the roll. The magnitude of such resistance depends on the direction of groove. The RD groove has the smallest resistance. Conversely, the TD grove has the largest one. The resistance of the 45-degree roll lies between the two. Imagining the surface resistance is useful in expecting the order of the type of roll.

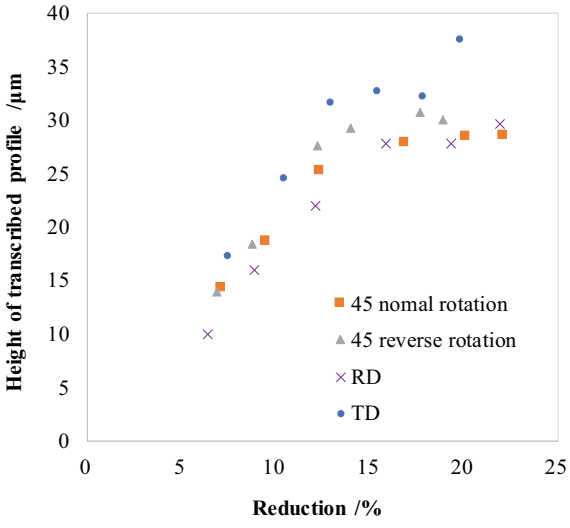

Fig. 5 Relation between rolling conditions and height of transcribed profile. (Color figure online)

3.2 *Estimation of Friction Coefficient*

The influence of the restraint force in the roll bite to be formed the projection height was suggested. To confirm the effect qualitatively, we estimated the friction coefficient during rolling on each roll as a macroscopic parameter. The method used to estimate the friction coefficient is described below. The sheet thickness on both the entry side and delivery side were measured under each condition.

Using the inverse equation of Hill's rolling load model, the estimated friction coefficient is shown in Eq. (1). However, flow stress k was estimated using Eq. (2). R' was calculated with Hitchcock's model using measured rolling load. Here, parameters A and n in Eq. (2) were determined using the fitting method taken from a great deal of experimental rolling data. As shown in Fig. 6, the estimated friction coefficients have strong dependency not only on reduction, but also on the type of roll. In general, the estimated friction coefficients increase as reduction increases. It is believed that there are two reasons for this increase. One is the new active surface, which is mainly formed by higher reduction. The other is the geometrical profile, which is shown in Fig. 3. It is difficult to explain these effects simply. We discuss this in detail in the following section.

$$\mu = \frac{\frac{P}{w\cdot\sqrt{R'\cdot(h1-h2)}\cdot(k-0.5\cdot(S1+S2))} + 1.02\cdot r - 1.08}{1.79\cdot r\cdot\sqrt{R'/h2}\cdot\sqrt{1-r}} \tag{1}$$

μ: friction coefficient P: rolling load w: width

R': flattening roll diameter $h1$: thickness of entry side $h2$: thickness of delivery side

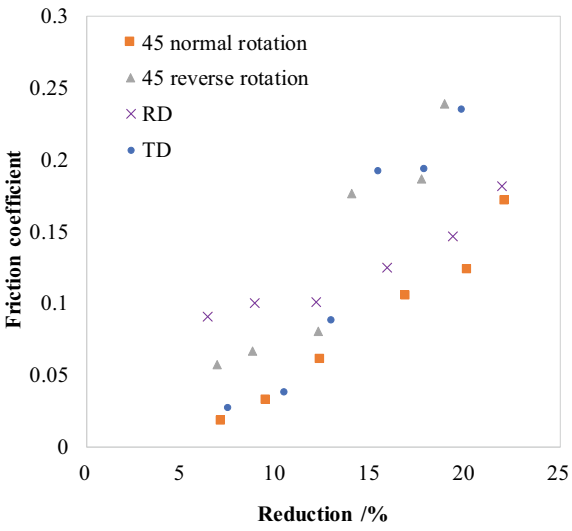

Fig. 6 Relation between reduction and friction coefficient. (Color figure online)

$S1$: tension of entry side $S2$: tension of delivery side
r: reduction k: flow stress

$$k = A \cdot \varepsilon^n \tag{2}$$

A: statical flow stress (112.7 kgf/mm^2) ε: strain n: work-hardening exponent (0.122).

4 Estimated Friction Coefficient at Each Roll

4.1 Friction of TD Groove Roll

A significant characteristic of the TD groove roll is that the friction coefficient shows an increased jump at around 15% reduction. In the TD groove roll, the geometrical distance between neighboring grooves is shorter along the rolling direction. If there is only one groove in the roll bite, the effect of the groove is limited. However, if there is more than one groove, the forward groove is highly resistant to the 2nd one. In evaluating this phenomenon, the contact length between the roll and the sheet was compared with the geometrical groove pitch. The relation between the friction coefficient and the ratio of these is shown in Fig. 7. In this figure, a jump in the friction coefficient exists around 2.0. This means that the number of grooves in the roll bite is important, and more than 2 grooves in the roll bite induce increasing resistance.

Previously, we examined the effect of the number of grooves in a roll bite on the friction coefficient and the height of transcribed profile by using 2D-FEA. The

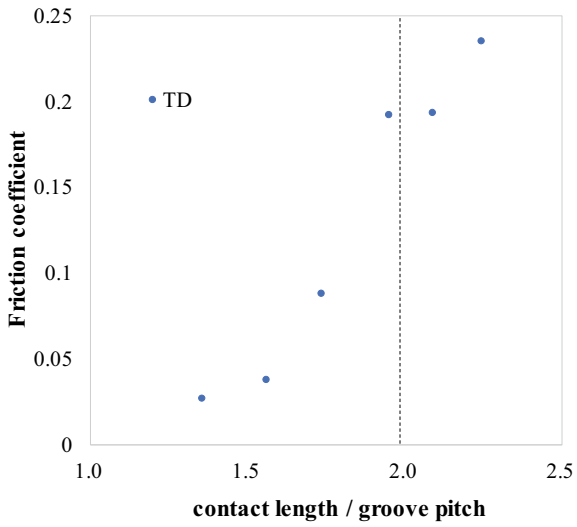

Fig. 7 Relation between rolling conditions and height of transcribed profile. (Color figure online)

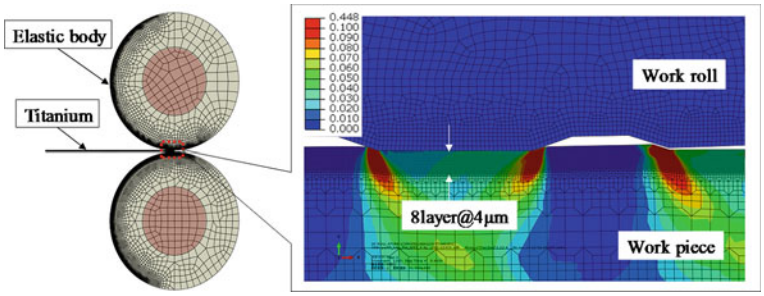

Fig. 8 2D-FEA model of rolling. (Color figure online)

Fig. 9 Relation between rolling conditions and friction coefficient and height of transcribed profile

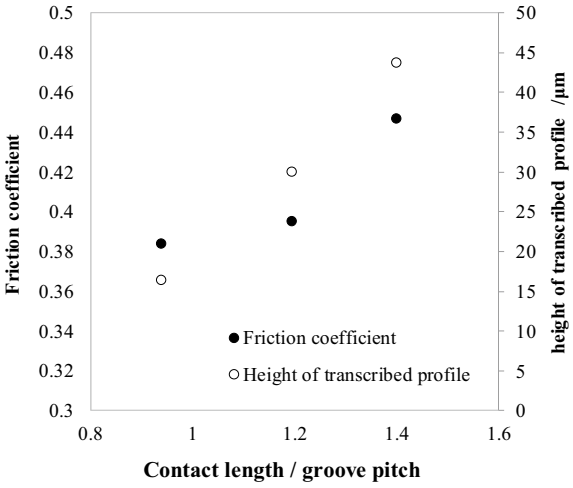

"ABAQUS-standard" in 2D-FEA was used for the simulations of the rolling test. The rolling model of the 2D-FEA is shown in Fig. 8 [7]. Figure 9 shows the relation between number of contact grooves and the friction coefficient from the 2D-FEA. The friction coefficient in the figure was estimated from Eq. (1) using the rolling load obtained from the 2D-FEA. As a result, it was confirmed that the apparent friction coefficient (restraint force) increased as the number of grooves in the roll bite increased. Also, it was clarified that the height of transcribed profile increased with the increase in the friction coefficient.

4.2 Friction Coefficient of 45-Degree Groove Roll

In the case of a 45-degree groove roll, there is a difference in estimated friction coefficients between normal and reverse rotation. The friction coefficient of reverse

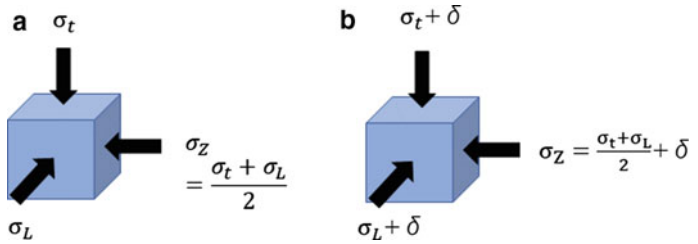

Fig. 10 Yield condition. **a** Plain strain. **b** Plain strain with additional stress δ. (Color figure online)

rotation is higher than in the case of normal rotation (Fig. 6). This difference is considered to be influenced by the lateral metal flow in the roll bite. In normal rotation, the metal flow along the rolling direction must be pushed outward from the center of the strip by the groove. On the other hand, in reverse rotation, the metal flow must be pushed toward the center from outside the groove.

These lateral metal flows along the width cause a compression stress along the width that is higher than in the case of normal rotation. Assuming Mises's yield criteria and associated flow rule, on the plane strain condition, yield condition is Eq. (3). σ_t is stress along the thickness, σ_L is stress along the rolling direction, σ_W is stress along the width direction and σ_{eq} is equivalent stress, as shown in Fig. 10a.

$$(\sigma_t - \sigma_L)^2 = \frac{2}{3}\sigma_{eq}^2 \tag{3}$$

If additional stress by constraint force along the width direction is assumed, the stress along the thickness is increased with compressive additional stress, and is decreased with stretch one as shown in Fig. 10b. As a result, the rolling load in reverse rotation is higher than in normal rotation. This is the reason why the estimated friction coefficient of reverse rotation is higher than in the other cases.

In addition, there is a jump phenomenon around 15%, as in the case of the TD groove roll. This jump might be the same phenomena as the TD groove roll. However, there is no jump in the case of a 45-degree normal rotation roll. This difference might come from the different axial metal flow between each other. In the case of reverse rotation, compressive flow along the width causes compressive stress along the rolling direction, too. On the other hand, in the case of normal rotation, the stretch flow along the width causes tensile stress along the rolling direction. This difference causes significant effect of the 2nd groove on the roll bit. In the case of normal rotation, the effect of the 2nd groove on the roll bite is very important, as it is in the case of the TD roll. However, in the case of normal rotation, the 2nd groove does not cause a strong compressive force, because of the axial metal flow from the center to the edge of the sheet. In Fig. 11, we show the heights of the transcribed projection at the center of the sheet and at the edge of the sheet with the 45-degree roll in both normal and reversed rotation. The height of the transcribed projections is higher in reverse than in normal rotation. Furthermore, this difference is quite large at the

Fig. 11 The height of the transcribed profile at the center of the sheet width and the edge. (Color figure online)

width edge portions in both normal and the reverse rotation. Since the free surface is formed at the width edge, the influence of the metal flow is large. It is presumed that the difference in compressive stress between normal rotation and reverse rotation appears in the height of the transcribed projection.

4.3 Relationship Between RD and TD Groove Roll

Figure 6 shows the estimated friction coefficients of the RD and the TD groove rolls with the reductions. As described above, the rapid increase in the friction coefficient at 15% or more with the TD groove roll is due to the resistance of the metal flow along the rolling direction. It is believed that the friction coefficient of the RD groove roll increases with higher reduction due to the formation of the new surface, which is in contact with the groove. Figure 12 shows the relationship between the friction coefficient and the contact area ratio of the protrusion and the roll bite length on the TD/RD rolls. In the RD roll, the contact area ratio is constant at any reduction. On the other hand, in the case of the TD roll, the contact area ratio increases with an increase in rolling reduction. The estimated friction coefficients are a kind of index of the resistance force along the rolling direction. Microscopic friction depends on the contact area ratio. If the microscopic friction is constant, the estimated friction is shown to relate to the contact area ratio in this figure. In particular, when more than two protrusions exist on the roll bite, it is believed that the restraining force in the rolling direction sharply increases and the friction coefficient jumps, as explained before.

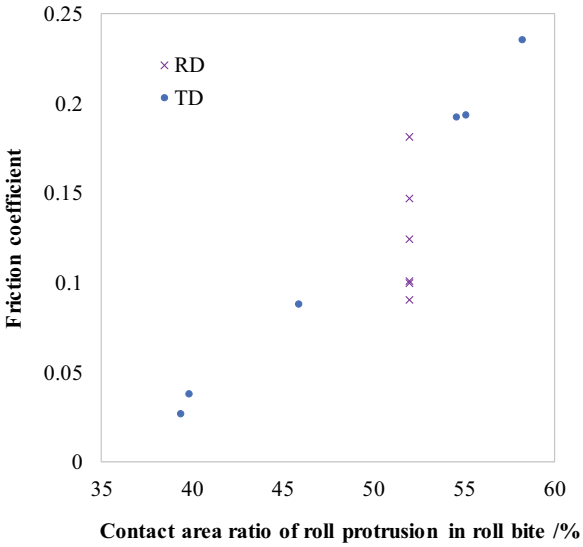

Fig. 12 Relationship between friction coefficient and contact ratio of roll protrusion. (Color figure online)

5 Relation Between Estimated Friction and Transcribed Profile

Figure 13 shows the relationship between the friction coefficient and the height of the projection for each roll.

In lower friction coefficients under 0.15, where the reduction is lower, it is difficult to understand the behavior of the friction coefficient because of the projection

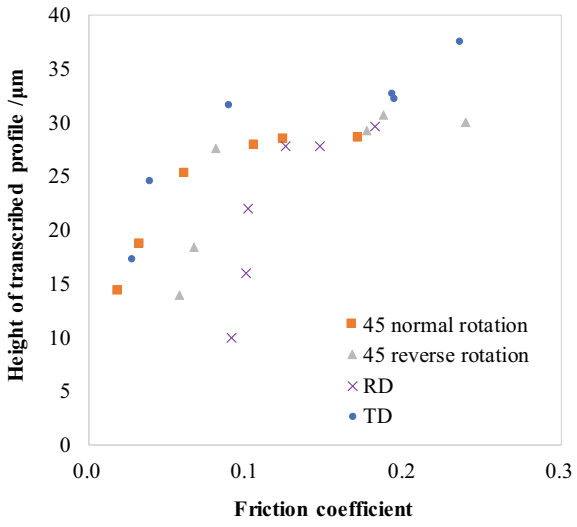

Fig. 13 Relationship between Height of transcribed profile and friction coefficient. (Color figure online)

formation process. In higher friction coefficients over 0.15, where the reduction is higher, higher friction causes higher projections with any of the rolls other than the 45-groove roll in reverse rotation. The compressive stress in the roll bite from the resistant force is helpful in forming the projection, as suggested other Refs. [8, 9]. In the case of the 45-degree groove roll in reverse rotation, an additional compressive stress along the width from the metal flow forces the formation of stronger flow stress on plan strain condition. This effect does not directly affect the resistant force. This might be the reason why a low projection height on the roll has a high friction coefficient.

6 Conclusion

To predict transferability on textured rolling, we have to decide on the adaptive boundary conditions, namely, the microscopic relative velocity between the material and the roll in the roll bite. Based on this idea, experimentally, we estimated the apparent friction coefficients of each roll (1) RD, (2) TD, and (3) the 45-degree groove roll. Based on our experiments, we confirmed that the influence of the following resistant forces exist in textured rolling.

1. Restraint force in the rolling direction due to the formation of protrusions
2. Restraint force in the rolling direction due to the presence of multiple roll grooves in the roll bite
3. Influence of flow stress due to metal flow in the width direction
4. Contact ratio of roll convex in the roll bite.

There is a relationship between the resistant force as the estimated friction coefficients and the projection height in the higher reduction area. However, the theoretical prediction itself of apparent friction coefficients is still difficult as there is an interaction between micro transferability and the resistant force. We conclude that it is important to estimate the apparent friction coefficient in predicting transferability.

References

1. Ataka M, Ueno Y, Watanuki K, Iino Y (2008) Tetsu-to-Hagané 94:63–69
2. Aoki I (1979) J Jpn Soc Technol Plast 20:1121–1125
3. Yukawa N, Akiyama T, Yoshida Y, Ishikawa T (2008) Analysis of surface roughness transcription in skin-pass rolling using zooming method. Iron Steel Inst Jpn 94(10):17–22
4. Ike H (2007) 3D Finite element analysis of surface roughness evolution of steel sheets by micro-indentation of surface asperities. Dev Micro-Deform Anal Pract Technol Temper Rolling Cold Rolled Steel Sheet 10:99–110
5. Fujii Y, Maeda Y (2006) Research of mechanism for surface texture by sheet rolling. In: The Proceedings of the 57th joint conference for the technology of plasticity, vol 215, pp 213–214
6. Fujii Y, Maeda Y (2007) Research of mechanism for surface texture by sheet rolling. In: IX international conference computational plasticity COMPLASIX, pp 787–790

7. Fujii Y, Maeda Y (2014) Proceedings of the international conference on the technology of plasticity, ICTP2014, pp 161–165
8. Akashi T, Shiraishi T, Ogawa S, Matsuse Y (2014) J Jpn Soc Technol Plast 55(639):324–330
9. Akashi T, Shiraishi T, Ogawa S, Matsuse Y, Morihara H (2015) J Jpn Soc Technol Plast 56(648):53–59